Gas Processing Journal
Vol. 5, No. 1, 2017
http://gpj.ui.ac.ir
DOI: 10.22108/GPJ.2017.100034.1000

Superstructure of Cogeneration of Power, Heating, Cooling and Liquid Fuels Using Gasification of Feedstock with Primary Material of Coal for Employing in LNG Process

Malek Shariati Niasar[1]*, Majid Amidpour[1], Bahram Ghorbani[2,3], Mohammad-Javad Rahimi[3], Mehdi Mehrpooya[4], Mohammad-Hossein Hamedi[3]

[1]Mechanical Engineering Faculty, Energy Systems Group, KNToosi University of Technology, Tehran, Iran

[2] Faculty of Engineering Technology, Amol University of Special Modern Technologies, Amol, Iran

[3] Mechanical Engineering Faculty, Energy Conversion Group, KNToosi University of Technology, Tehran, Iran

[4] Renewable Energies and Environmental Department, Faculty of New Sciences and Technologies, University of Tehran, Tehran, Iran

Article History
Received: 2016-11-02 Revised: 2017-06-07 Accepted: 2017-08-24

Abstract
Using absorption refrigeration cycles instead of vapor compression refrigeration cycles can drastically decrease energy consumption. In these systems, high level of energy consumption is reduced due to the partially elimination of vapor compression refrigeration systems. On the other hand, utilization of waste heat of the plant, which is a very good opportunity for energy saving, is possible. In the present paper, a novel mixed fluid cascade natural gas liquefaction process is investigated by exergy and exergoeconomic analysis methods. In this process, one of the vapor compression cycles is replaced by water-ammonia absorption refrigeration cycle. The simulation results show that the compressors of this plant are responsible for 43.2% of total exergy lost. Decision variables of the system are consists of mass flow ratio of the tower's bottom product (bottom feed ratio), number of trays, and compressor's pressure ratio. Choosing appropriate values for these variables will result in 12% increase in exergetic efficiency of the plant. Exergoeconomic factor of water coolers, heat exchanger no.1 and tower no.1 shows that these components respectively impose a sizable capital cost to the entire system and does not result to a reasonable capital recovery. In this paper an integrated structure of producing liquid fuels from coal using Fischer-Tropsch synthesis and some equipment such as gas and steam turbines as well as HRSG heat exchanger for recovering of heat and power has been developed. Gasification method because of high efficiency and exothermic nature from energy consumption point of view is employed for producing synthesis gas.

Keywords
Cogeneration, Natural Gas Liquids (LNG), Gasification, Exergoeconomic

1. Introduction

Liquefied natural gas (LNG) is natural gas in a liquid form that is clear, colorless, odorless, noncorrosive, and nontoxic, occupying only 1/600th of its normal volume in gaseous form. LNG is formed when natural gas is cooled by a refrigeration process to temperatures of between 159 ºC and –162 ºC through a process known as liquefaction (Bahadori, 2014). Today, natural gas, often supplied as LNG, is particularly well-suited for use in the combined cycle technology used in independent power generation projects (IPPs). LNG has established a niche for itself by matching remote gas supplies to markets that lacks indigenous gas

* **Corresponding Author.**
Authors' Email Address:
[1] **M. Shariati Niasar** (malekniassar@gmail.com), [2] **Majid Amidpour** (amidpour@kntu.ac.ir), [3] **Bahram Ghorbani (b.ghorbani@ausmt.ac.ir)**, **Mohammad-Javad Rahimi** (mohamad_rah@yahoo.com), [4] **Mehdi Mehrpooya (mehrpoya@ut.ac.ir)**, [5] **Mohammad-Hossein Hamedi(hamedi@kntu.ac.ir)**[6]

ISSN (Online): 2345-4172, **ISSN (Print):** 2322-3251

reserves (Avidan, Gardner, Nelson, Borrelli, & Rethore, 1997). High amount of energy is needed to liquefy and sub-cool the natural gas to temperatures around -160 ºC. In general, compressors of the refrigeration cycles are the biggest energy consumer of the liquefaction process. In fact, the electrical power required for compression refrigeration cycles (CRCs) is the highest energy sink of the plant. In order to define the efficiency of the natural gas liquefaction (NGL) process, an index named specific power consumption (SPC) is introduced. This index expresses the amount of the required power (kWh) to produce 1 kg of LNG. According to reference (Waldmann, 2008) SPC varies from 0.3 to 0.8 (kWh/Kg LNG). Several researches have been conducted to improve efficiency of NGL processes. Mixed fluid cascade (MFC) process is a technology, which has been developed to reduce the power required for LNG production. The MFC process is highly efficient due to the use of the three mixed refrigerant cycles, each with different compositions, which result in minimum compressor shaft power (Berger, Forg, Heiersted, & Paurola, 2003). The mixed fluid cascade (MFC) LNG process is developed by The Statoil Linde Technology Alliance. MFC process is studied from several points of view in literature. The study of the degrees of freedom of MFC process and how to adjust key variables to achieve optimal steady state operation is conducted in an investigation (Jensen & Skogestad, 2006). An invention relates to a method for liquefying a stream rich in hydrocarbons, by the indirect exchange of heat with the refrigerants in a closed-circuit cascade of mixed refrigerants. According to the invention, 3 circuits of mixed refrigerants are employed with each circuit comprising different refrigerants. The three circuits are used for pre-cooling, liquefying and super-cooling the hydrocarbon-rich stream (Stockmann et al., 2001). Optimization of the refrigeration systems has drawn a lot of attention. Several parameters are chosen for optimization by so many researchers as presented in (Amidpour et al., 2015; Ghorbani, Hamedi, Shirmohammadi, Mehrpooya, & Hamedi, 2016; Ghorbani, Mafi, Shirmohammadi, Hamedi, & Amidpour, 2014; Salomón, Gomez, & Martin, 2013; Shirmohammadi, Ghorbani, Hamedi, Hamedi, & Romeo, 2015). Genetic algorithm (GA) method coupled with the process simulation software Aspen Plus is used to optimize mixed refrigerant composition solution under different cold box inlet temperatures. The results show that when the ambient temperature increases, the concentrations of methane, ethylene and propane should decrease, and isopentane should increase (Xu, Liu, Jiang, & Cao, 2013). A generalized model for the compressor operations in multiple interacting refrigerant cycles in LNG applications is presented and the optimal load distribution between the cycles is selected to minimize total power consumption of the system (M. F. Hasan, Razib, & Karimi, 2009). The optimal operating conditions for a Dual Mixed Refrigerant (DMR) cycle are determined by considering the power efficiency. For this purpose, a mathematical model for (DMR) cycle is formulated and the optimal operating conditions from the formulated mathematical model is obtained using a hybrid optimization method that consists of the genetic algorithm (GA) and sequential quadratic programming (SQP) (Hwang, Roh, & Lee, 2013). Genetic algorithm (GA) is used to optimize a propane pre-cooled mixed refrigerant LNG plant with 22 variables and 24 constraints. New refrigerant mixtures is found, with savings in power consumption as high as 13.28%, in fact, The optimized LNG plant model consumes 100.78 MW, whereas the baseline consumes 110.84 MW (Alabdulkarem, Mortazavi, Hwang, Radermacher, & Rogers, 2011). Operating pressure of the cycles is used for the optimization process in reference (M. Hasan, Karimi, & Alfadala, 2009). Certain thermodynamic aspects of cryogenic turbines, which are intended to produce power in NGL plant by replacing the throttling valves, are investigated based on operational data provided by a cryogenic test facility (Kanoğlu, 2001). Energetic, exergetic and advanced exergetic analysis are performed for five mixed refrigerant LNG processes to identify the potentials and strategies to improve thermodynamic performance of these energy intensive processes. Exergy analysis results showed that the maximum exergy efficiency is related to the MFC process(Ghorbani, Hamedi, Shirmohammadi, Hamedi, & Mehrpooya, 2016). A techno-economic assessment, also presented in (Petrakopoulou, Tsatsaronis, & Morosuk, 2013) as exergoeconomic analysis, has been carried out for the liquefied natural gas (LNG) production facilities in western Canada (Raj, Suman, Ghandehariun, Kumar, & Tiwari, 2016). Exergy analysis of biogas production from a municipal solid waste landfill has been investigated (Xydis, Nanaki, & Koroneos, 2013). Energy and environmental evaluation have been carried out for Small-scale biomass gasification CHP utilization in industry (Adams & McManus, 2014). Economic and CO2 avoided emissions analysis of wastewater treatment

plant have been carried out for biogas recovery and its usage in a small power plant in Brazil (dos Santos et al., 2016). Techno-economic analysis has been employed for evaluation of an integrated biogas based poly-generation (Khan, Mainali, Martin, & Silveira, 2014).

Increasing the efficiency of the liquefaction process by the use of available waste heat from parts of the plant is a potential opportunity for process improvement (Alabdulkarem et al., 2011; Dispenza, La Rocca, Messineo, Morale, & Panno, 2013). Using an absorption–refrigeration system (ARS) to convert waste heat into useful cooling energy can improve energy efficiency(Ghorbani, Hamedi, Amidpour, & Shirmohammadi, 2017). The application of ARSs reduces the electricity consumption of conventional vapor compression refrigerators, but such traditional compression systems still dominate the market. In ARSs, two working fluids are used as refrigerant and absorbent. Water lithium bromide (H2O–LiBr) and ammonia–water (NH3–H2O) are commercially available throughout the world (Han et al., 2013; Wang & Oliveira, 2006; Yan, Chen, Hong, Lin, & Tang, 2013). Several researches have shown that this technology is helpful in so many industries (Aneke, Agnew, Underwood, & Menkiti, 2012; Brant, Brueske, Erickson, & Papar, 1998; Bruno, Vidal, & Coronas, 2006; Ghaebi, Karimkashi, & Saidi, 2012; Táboas, Bourouis, & Vallès, 2014). For example in a Combined Heat and Power (CHP) plant, R-curve concept is used to integrate an absorption chiller into the total site for utilizing its cooling production (Ghaebi et al., 2012). Improving the efficiency of LNG plants with the use of ACR is an important research field, which has drawn a lot of attention. Enhancement of LNG plant propane cycle is done through waste heat powered absorption cooling (Mortazavi, Somers, Alabdulkarem, Hwang, & Radermacher, 2010; Rodgers et al., 2012). The usage of an absorption refrigeration system powered by waste heat from gas turbine is investigated. This method provides the necessary cooling at reduced overall energy consumption compared with CRC. The results showed that recovering waste heat from a 9 megawatts (MW) gas turbine could save 1.9 MW of electricity consumption (Kalinowski, Hwang, Radermacher, Al Hashimi, & Rodgers, 2009). A novel configuration for large-scale natural gas liquefaction process is introduced and analyzed based on replacement of vapor compression refrigeration cycle by absorption refrigeration system. the results show that specific power consumption of the introduced process is 0.172 kWh/kgLNG which shows 30 % reduction in the power consumption (Mehrpooya, Omidi, & Vatani, 2016).

In this study, intrinsic and induced malfunctions of the components are analyzed and quantified. Exergetic, exergoeconomic and exergoenvironmental analyses are applied on PRICO liquefaction process (Morosuk, Tesch, Hiemann, Tsatsaronis, & Bin Omar, 2015). Options for improving the PRICO process and the application of exergy-based methods to improve an LNG plant are discussed. A double effect absorption refrigeration system is investigated and a comparative analysis is performed based on the exergy destruction for different heat sources (Kaynakli, Saka, & Kaynakli, 2015). Exergoeconomic evaluation of an integrated co-production processes based on the MFC and absorbtion refrigeration systems has been developed (Ghorbani, Hamedi, & Amidpour, 2016).

A novel mixed fluid cascade natural gas liquefaction process, which employs absorption refrigeration system, is analyzed by exergy and exergoeconomic analysis methods. Specification of the process is introduced and analyzed in (Mehrpooya et al., 2016). In the first step, exergy efficiency and exergy destruction of the process components are calculated. In the next step, all of the equipment are sized and costs of them are calculated with a suitable cost function. Mathematical modeling of the process is done in order to find the exergoeconomic factors. Finally, exergoeconomic variables, exergy destruction cost, relative cost difference and exergoeconomic factor are computed.

2. Process Description and System Configuration

The MFC process is consists of three pure refrigerants that have different boiling temperatures, such as methane, ethylene, and propane. First, natural gas is cooled to -25 ºC in the propane cycle, and then it is cooled to -86 ºC in the ethylene cycle. Finally, it is liquefied to -160 ºC in the methane cycle. The MFC process is highly efficient due to the low shaft power consumption of the three MRC compressors(Bahadori, 2014). A schematic diagram of the proposed MFC process is shown in figure1.

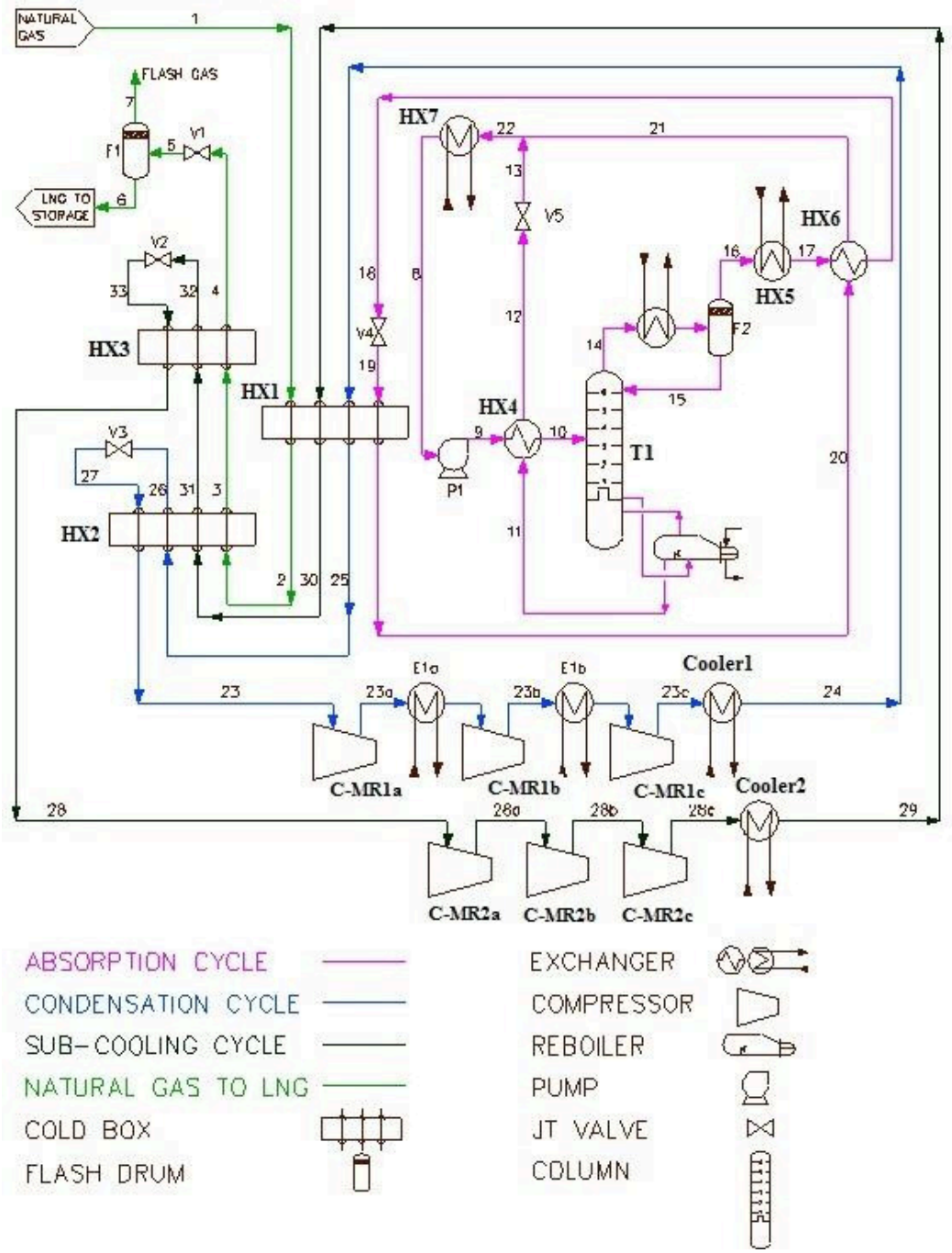

Figure 1. Schematic flow diagram of the modified MFC process

It can be seen in Fig.1 that refrigerant experience an increase in pressure and temperature as it passes through the compression system. Next, the refrigerant, which is hot and has high pressure, passes through the condenser and is condensed. Water from an external source is used to cool the refrigerant in the condenser. A throttling valve is used to decrease temperature and pressure of refrigerant. In the next stage, NG and refrigerant of the previous refrigeration cycle is cooled in the cold box with the aid of cold, low-pressure refrigerant. Finally, the hot refrigerant returns back to the compressor. The simulation process is done with the aid of available information from (Venkatarathnam & Timmerhaus, 2008) using Soave-Redlich-KWong (SRK) thermodynamic equation of state. The results of simulation are fully compatible with the data in (Venkatarathnam & Timmerhaus, 2008).

In the proposed modified MFC process, a NH3/ H2O absorption refrigeration system is used instead of the first compression refrigeration cycle, but other compression refrigeration cycles are remained unchanged.

More detail description about the process can be found in (Mehrpooya et al., 2016). Table 1 presents the thermodynamic data for the material streams of the process.

Table 1. Thermodynamic specifications of the modified MFC process

Stream no.	Temperature (C)	Pressure (bar)	Flow (kg.mol/h)	Physical exergy (kW)	Chemical exergy (kW)	Total exergy (kW)
1	26.85	65	6771	18666	1664325	1682992
2	-25.25	65	6771	12241	1664325	1683478
3	-85.35	65	6771	24170	1664325	1688496
4	-160.15	65	6771	32775	1664325	1697101
5	-166.1	1	6771	31526	1664325	1695852
6	-166.1	1	6303	30813	1596265	1627078
7	-166.1	1	468	469	68304	68774
8	31.39	1.2	53620	1563	1345297	1345799
9	31.98	1.3	53620	94	1345297	1345391
10	122.85	13	53620	18181	1345297	1363401
11	146.18	13	47358	21363	7543942	786139
12	36.98	13	47358	593	754394	754987
13	37.23	1.2	47358	259	754394	754653
16	45.48	13	6261	10602	593004	603607
17	33.97	13	6261	9528	593004	602533
18	-24.42	13	6261	10141	593004	603146
19	-29.55	1.2	6261	10060	593004	603065
20	-29.42	1.2	6261	2302	593004	595307
21	13.05	1.2	6261	738	593004	593742
22	45.82	1.2	53620	2432	593004	1347858
23	-24.35	3.1	6927	5714	1345297	2995718
24	36.85	27.9	6927	14766	2990004	3004771
25	-21.49	27.9	6927	16586	2990004	3006590
26	-78.48	27.9	6927	19725	2990004	3009729
27	-90.27	3.1	6927	19038	2990004	3009042
28	-87.68	3.5	4882	5542	1224039	1229582
29	36.85	33.9	4882	11473	1224039	1235512
30	-21.29	33.9	4882	11705	1224039	1235743
31	-83.28	33.9	4882	15788	1224039	1239827
32	-154.05	33.9	4882	22649	1224039	1246688
33	-163.15	3.5	4882	22021	1224039	1246060
34	25	1.013	493703	121	427876	427997
35	30	1.013	493703	440	427876	428316
36	25	1.013	493703	234	285477	285711
37	30	1.013	493703	393	285477	285871

3. Exergy Analysis

Exergy is a measure of the maximum capacity of a system to perform useful work as it proceeds to a specified final state in equilibrium with its surroundings. Exergy is generally not conserved as energy, but destructed in the system. Exergy destruction is the measure of irreversibility that is the source of performance loss. Therefore, an exergy analysis assessing the magnitude of exergy destruction identifies the location, the magnitude and the source of thermodynamic inefficiencies in a thermal system (Dai, Wang, & Gao, 2009).

In table1 physical and chemical exergy of the process material streams as well as their temperature, pressure and mass flow rate are presented. It should be noted that calculation of standard chemical exergy of the hydrocarbon streams is down based on the relations which are developed in(Sheikhi, Ghorbani, Shirmohammadi, & Hamedi, 2014, 2015). Also the data set for the standard chemical exergy of the other components is obtained from (Kotas, 2013).

In table 2, exergy efficiencies of the process components are calculated using exergy balance equations of the components. For this purpose, physical and chemical exergy of input fuel and output products as well as exergy loss and irreversibilities are computed.

In this study $\dot{E}_F$, $\dot{E}_P$ and $\dot{E}_D$, are defined as the fuel exergy rate, the product exergy and the exergy destruction rate, respectively. The exergy balance over the k_{th} component is

$$\dot{E}_{F,k} = \dot{E}_{P,k} + \dot{E}_{D,k} \quad (1)$$

y_k (ratio of exergy destruction) is defined as:

$$y_k = \frac{\dot{E}_{D,k}}{\dot{E}_{F,tot}} \quad (2)$$

Table 2 presents the definitions used for calculation of exergy efficiency of the process component. In addition, exergy efficiency of the process components is listed in this table.

Table 2. Definitions for exergy efficiencies of the process components

Components and exergy efficiency expression	Component identifier	Exergy efficiency (%)	Component identifier	Exergy efficiency (%)
Heat Exchanger	HX-1	84.93	HX-5	97.8
	HX-2	96.65	HX-6	88.46
	HX-3	93.78	HX-7	92.67
	Hx-4	97.35		
Compressor and Pump	C-MR1	82.21	C-MR2	83.86
	Pump1	0.3		
Expansion valve	V-1	30.29	V-4	22.91
	V-2	55.72	V-5	51.63
	V-3	55.32		
Cooler	Cooler1	88.9	Cooler2	83.77
Column	T1	81		

4. Exergoeconomic Analysis

4.1. Economic Model

Combining the economics principles with the second law of thermodynamics results in exergoeconomic analysis method. In this method, cost value of the exergy for each stream is determined. Based on the cost value of the streams cost of the components inefficiencies can be calculated and discussed (Bejan A, 1996). Total Revenue Requirement (TRR) method is used in this study for economic analysis. The detail description about the economic model and its terms can be found in (Bejan A, 1996). Economic constants and assumptions are displayed in table 3.

Table 3. Economic constants and assumptions

Economic parameters	Value
Average annual rate of the cost of money (i_{eff})	10%
Average nominal escalation rate for the operating and maintenance cost (r_{OMC})	5%
Average nominal escalation rate for fuel (r_{FC})	5%
Plant economic life (book life)	25 years
Total annual operating hours of the system operation at full load	7300

The levelized annual total revenue requirement (TRR_L) is calculated as follows with the aid of Capital Recovery Factor (Bejan A, 1996):

$$TRR_L = CRF \sum_{1}^{BL} \frac{TRR_j}{(1+i_{eff})^j} \quad (3)$$

CRF is calculated according to the following equation:

$$CRF = \frac{i_{eff}(1+i_{eff})^{BL}}{(1+i_{eff})^{BL}-1} \quad (4)$$

TRR_j is sum of four annual terms including return on investment (ROI), total capital recovery (TCR), operation and maintenance costs (OMC) and fuel costs (FC) as it is mentioned in (Bejan A, 1996).

$$TRR_j = TCR_j + ROI_j + FC_j + OMC_j \quad (5)$$

Cost of electricity during j^{th} year is calculated as follows:

$$FC_j = FC_0(1+r_{FC})^j \quad (6)$$

FC_0 is fuel cost at the starting point year. It is calculated as below:

$$FC_0 = c_w \times \dot{W} \times \tau \quad (7)$$

Where:

τ = total annual time (in hours) that is 7300 h year^{-1}

C_w = unit cost of fuel (0.071 \$ kWh^{-1})

$\dot{W}$ = power (kW)

The levelized annual operating and maintenance costs OMC_L are calculated as follows:

$$OMC_L = OMC_0 \times CELF = OMC_0 \frac{k_{OMC}(1-k_{OMC}^{BL})}{(1-k_{OMC})} CRF \quad (8)$$

Where:

$$k_{OMC} = \frac{1+r_{OMC}}{1+i_{iff}} \qquad r_{OMC} = \text{constant} \quad (9)$$

r_{OMC} is the annual escalation rate for the operating and maintenance costs. The levelized carrying charges CC_L is calculated as follows:

$$CC_L = TRR_L - FC_L - OMC_L \quad (10)$$

Based on the components purchased cost, capital investment $\dot{Z}_k^{CI}$ and operating and maintenance costs $\dot{Z}_k^{OM}$ of the total plant are gained.

$$\dot{Z}_k^{CI} = \frac{CC_L}{\tau} \frac{PEC_k}{\sum_k PEC_k} \quad (11)$$

$$\dot{Z}_k^{OM} = \frac{OMC_L}{\tau} \frac{PEC_k}{\sum_k PEC_k} \quad (12)$$

Where, τ and PEC_k are the total annual hours of plant operation and the purchased-equipment cost of the k^{th} component, respectively. $\dot{Z}_k$ is the cost rate associated with the capital investment and operating and maintenance costs:

$$\dot{Z}_k = \dot{Z}_k^{CI} + \dot{Z}_k^{OM} = \frac{CC_L + OMC_L}{\tau} \frac{PEC_k}{\sum_k PEC_k} \quad (13)$$

Rate of levelized costs is computed according to the following equation:

$$\dot{C}_F = \frac{FC_L}{\tau} \quad (14)$$

Table 4 and 5 respectively show the cost functions used for calculation of the process equipment cost and the purchased equipment and investment costs.

Table 4. Purchased cost of equipment.

Component	Purchased equipment cost functions
Compressor	$C_C=7.90(HP)^{0.62}$ C_C= Cost of Compressor (k$)
Heat exchanger	$C_E=a(V)^b+c$ C_E= Cost of Heat exchanger ($)
Pump	$C_P=f_M f_T C_b$ C_P= Cost of Pump ($) $C_b=1.39\exp[8.833-0.6019(\ln Q(H)^{0.5})+0.0519(\ln Q(H)^{0.5})^2]$, Q in gpm, H in ft head f_M= Material Factor $f_T=\exp[b_1+b_2(\ln Q(H)^{0.5})+b_3(\ln Q(H)^{0.5})^2]$ b_1= 5.1029, b_2= -1.2217, b_3= 0.0771
Drum	$C_D=f_m C_b+C_a$ C_D= Cost of Drum ($) $C_b=1.218\exp[9.1-0.2889(\ln W)+0.04576(\ln W)^2]$, 5000<W<226000 lb shell weight $C_a=300D^{0.7396}L^{0.7066}$, 6<D<10, 12<L<20 ft f_m= Material Factor
Cooler	$C_C=1.218k(1+fd+fp)Q^{0.86}$, 20<Q<200 M BTU/hr C_C= Cost of cooler ($) f_m=Design Type f_P=Design Pressure (psi) a=0.4692, b=0.1203, c=0.0931
Absorber	$C_b=1.128\exp(6.629+0.1826(\log W)+0.02297*(\log W)^2)$ $C_{p1}=300(D^{0.7395})(L^{0.7068})$ $C_1=1.218[(1.7C_b+23.9V1+Cp1)]$ C_2=Cost of installed manholes, trays and nozzles C_3= Cost ofCooler C_4= Cost of Heater $C_{Ab}=C_1+C_2+C_3+C_4$ C_{Ab}= Cost of Drum ($)

Table 5. Purchased equipment and investment costs of process components

	PEC ($\times 10^3$ $)	Z^{CI} ($/hr)	Z^{OM} ($/hr)	Z ($/hr)
HX-1	170.99	18.61	0.4	19.01
HX-2	34.11	3.71	0.08	3.79
HX-3	43.53	4.74	0.10	4.84
HX-4	38.21	4.19	0.09	4.28
HX-5	38.36	4.16	0.09	4.25
HX-6	38.41	4.2	0.09	4.29
HX-7	38.9	4.17	0.09	4.26
Cooler1	10.37	0.04	0.006	0.046
Cooler2	10.39	0.04	0.003	0.043
C-MR1	2508.32	272.93	5.86	278.78
C-MR2	3406.15	370.62	7.95	378.57
Pump1	89.98	9.79	0.21	10
D-1	10.43	0.16	0.01	0.16
T1	5220.84	568.07	12.19	580.26

4.2. Cost Balance Equations

The cost balance equation expresses that the cost rate associated with the "product" of the system equals the total rate of expenditures made to generate the product, namely the "fuel" cost rate, and the cost rate associated with capital investment and operating and maintenance. For each component of the system, operating at a steady state, a cost balance equation is written.

Cost balance equation for the K_{th} component of the system is as follows:

$$\sum_i (c_i \dot{E}_i)_k + \dot{Z}_k^{CL} + \dot{Z}_k^{OM} = \sum_o (c_o \dot{E}_o)_k \quad (15)$$

$\dot{Z}_k^{CI}$, $\dot{Z}_k^{OM}$ are primary investment cost and the operation and maintenance cost respectively. components which have more than one output, some auxiliary equations should be written too (Bejan A, 1996). So based on the cost balances and auxiliary equations for all components a set of linear equations is gained as follows:

$$[\dot{E}_k] \times [c_k] = [\dot{Z}_k] \quad (16)$$

Where $[\dot{E}_k]$, $[c_k]$ and $[\dot{Z}_k]$ are exergy rate matrix, costs per unit of exergy vector and coefficient vector for $\dot{Z}_k$, respectively. Table 6 shows the cost balance and auxiliary equations for the process components.

Table 6. Main and auxiliary equations for the equipment

Equip.	Main Equation	Auxiliary Equation
HX-1	$\dot{C}_{19} + \dot{C}_{24} + \dot{C}_{29} + \dot{C}_1 + \dot{Z}_{HX-1} = \dot{C}_{20} + \dot{C}_2 + \dot{C}_{30} + \dot{C}_2$	$\frac{\dot{C}_{20}}{\dot{E}_{20}} = \frac{\dot{C}_{19}}{\dot{E}_{19}}$, $\frac{\dot{C}_{25} - \dot{C}_{24}}{\dot{E}_{25} - \dot{E}_{24}} = \frac{\dot{C}_{30} - \dot{C}_{29}}{\dot{E}_{30} - \dot{E}_{29}} = \frac{\dot{C}_2 - \dot{C}_1}{\dot{E}_2 - \dot{E}_1}$
HX-2	$\dot{C}_2 + \dot{C}_{30} + \dot{C}_{25} + \dot{C}_{27} + \dot{Z}_{HX-2} = \dot{C}_3 + \dot{C}_{31} + \dot{C}_{26} + \dot{C}_{23}$	$\frac{\dot{C}_{23}}{\dot{E}_{23}} = \frac{\dot{C}_{27}}{\dot{E}_{27}}$, $\frac{\dot{C}_3 - \dot{C}_2}{\dot{E}_3 - \dot{E}_2} = \frac{\dot{C}_{31} - \dot{C}_{30}}{\dot{E}_{31} - \dot{E}_{30}} = \frac{\dot{C}_{26} - \dot{C}_{25}}{\dot{E}_{26} - \dot{E}_{25}}$
HX-3	$\dot{C}_3 + \dot{C}_{31} + \dot{C}_{33} + \dot{Z}_{HX-3} = \dot{C}_4 + \dot{C}_{32} + \dot{C}_{28}$	$\frac{\dot{C}_{28}}{\dot{E}_{28}} = \frac{\dot{C}_{33}}{\dot{E}_{33}}$, $\frac{\dot{C}_4 - \dot{C}_3}{\dot{E}_4 - \dot{E}_3} = \frac{\dot{C}_{32} - \dot{C}_{31}}{\dot{E}_{32} - \dot{E}_{31}}$
HX-4	$\dot{C}_9 + \dot{C}_{11} + \dot{Z}_{HX-4} = \dot{C}_{10} + \dot{C}_{12}$	$\frac{\dot{C}_{11} - \dot{C}_{12}}{\dot{E}_{11} - \dot{E}_{12}} = \frac{\dot{C}_9 - \dot{C}_{10}}{\dot{E}_9 - \dot{E}_{10}}$
HX-5	$\dot{C}_{16} + \dot{C}_{36} + \dot{Z}_{HX-5} = \dot{C}_{17} + \dot{C}_{37}$	$\frac{\dot{C}_{16} - \dot{C}_{17}}{\dot{E}_{16} - \dot{E}_{17}} = \frac{\dot{C}_{36} - \dot{C}_{37}}{\dot{E}_{36} - \dot{E}_{37}}$
HX-6	$\dot{C}_{17} + \dot{C}_{20} + \dot{Z}_{HX-6} = \dot{C}_{21} + \dot{C}_{18}$	$\frac{\dot{C}_{18} - \dot{C}_{17}}{\dot{E}_{18} - \dot{E}_{17}} = \frac{\dot{C}_{20} - \dot{C}_{21}}{\dot{E}_{20} - \dot{E}_{21}}$
HX-7	$\dot{C}_{22} + \dot{C}_{water,in} + \dot{Z}_{HX-7} = \dot{C}_8 + \dot{C}_{water,out}$	None
C-MR1	$\dot{C}_{28} + \dot{C}_{W1} + \dot{Z}_{C-MR4} = \dot{C}_{28a}$	None
C-MR2	$\dot{C}_{23} + \dot{C}_{W2} + \dot{Z}_{C-MR2} = \dot{C}_{23a}$	None
Pump1	$\dot{C}_8 + \dot{C}_{W100} + \dot{Z}_{Pump} = \dot{C}_9$	None
Cooler1	$\dot{C}_{28a} + \dot{C}_{Q1} + \dot{Z}_{Cooler1} = \dot{C}_{29}$	None
Cooler2	$\dot{C}_{23a} + \dot{C}_{Q2} + \dot{Z}_{Cooler2} = \dot{C}_{24}$	None
D-1	$\dot{C}_5 + \dot{Z}_{D-1} = \dot{C}_6 + \dot{C}_7$	$\frac{\dot{C}_6}{\dot{E}_6} = \frac{\dot{C}_7}{\dot{E}_7}$
Tower	$\dot{C}_{10} + \dot{C}_{Q3} + \dot{Z}_{T1} = \dot{C}_{16} + \dot{C}_{11}$	$\frac{\dot{C}_{16}}{\dot{E}_{16}} = \frac{\dot{C}_{11}}{\dot{E}_{11}}$
V-1	$\dot{C}_4 = \dot{C}_5$	None
V-2	$\dot{C}_{32} = \dot{C}_{33}$	None
V-3	$\dot{C}_{26} = \dot{C}_{27}$	None
V-4	$\dot{C}_{12} = \dot{C}_{13}$	None
V-5	$\dot{C}_{18} = \dot{C}_{19}$	None

4.3. Exergoeconomic Variables

$\dot{E}_F$ and $\dot{E}_p$ are defined respectively fuel and product exergy rate for a component. On this basis, $\dot{C}_F$ and $\dot{C}_P$ are fuel cost rate and product cost rate respectively. In addition, for k_{th} component of the system $c_{F,k}$ is average cost per unit of exergy of fuel according to the below equation.

$$c_{F,k} = \frac{\dot{C}_{F,k}}{\dot{E}_{F,k}} \quad (17)$$

In this way, product average cost per unit of exergy and cost of exergy destruction, for the k_{th} component are defined as:

$$c_{P,k} = \frac{\dot{C}_{P,k}}{\dot{E}_{P,k}} \quad (18)$$

$$\dot{C}_{D,k} = c_{F,k}\dot{E}_{D,k} \quad (19)$$

Relative cost difference is also defined as follows:

$$r_k = \frac{c_{P,k} - c_{F,k}}{c_{F,k}} = \frac{1-\varepsilon_k}{\varepsilon_k} + \frac{\dot{Z}_k}{c_{F,k}\dot{E}_{P,k}} \quad (20)$$

Exergoeconomic factor is the ratio of investments cost to the total investment plus cost of exergy destruction. It is computed with following equation:

$$f_k = \frac{\dot{Z}_k}{\dot{Z}_k + \dot{C}_{D,k}} \quad (21)$$

5. Results and Discussion

5.1. Results of Exergy Analysis

With reference to the Fig.2, it can be seen that among all equipment, heat exchangers have the highest efficiency. HX-5 and HX-4 have the highest efficiencies (97.8% and 97.35% respectively). In addition, C-MR2 and C-MR1 have the highest efficiencies among all compressors of the system (83.86% and 82.1% respectively).

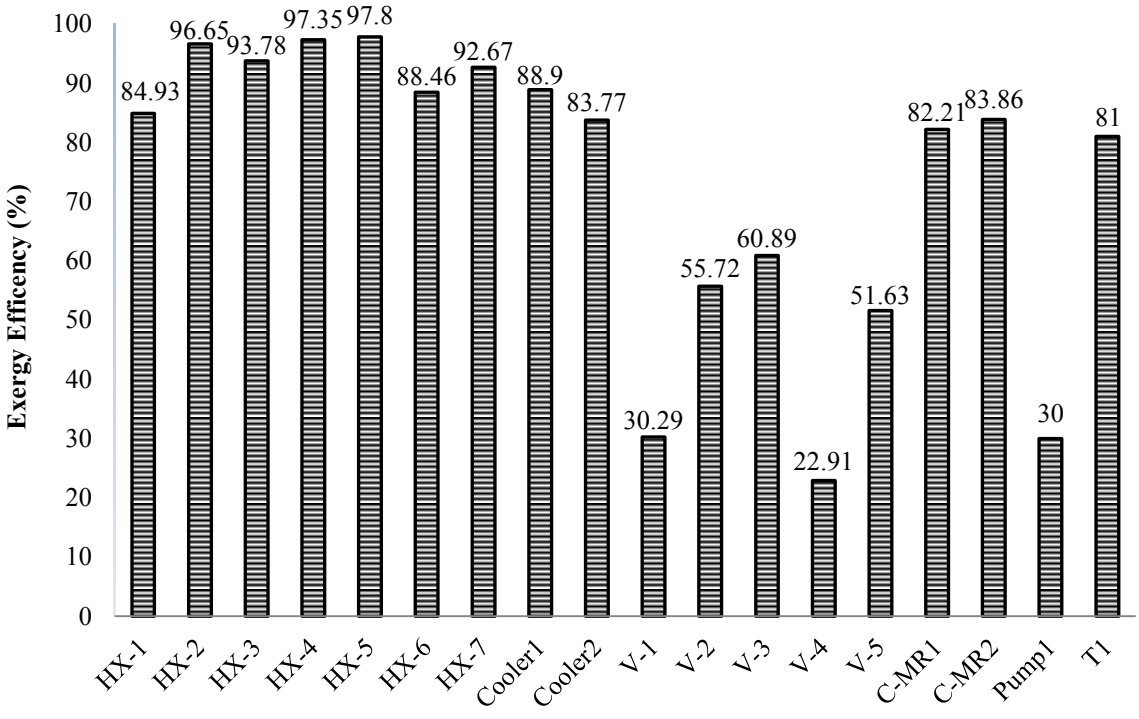

Figure 2. Exergy efficiencies of the Modified MFC process

As it is observed in Fig.3, the major exergy destructions occur in the compressors. Actually, the compressors are responsible for almost 43.2% of the total exergy destruction. C-MR2 with 17727kW has the highest exergy destruction.

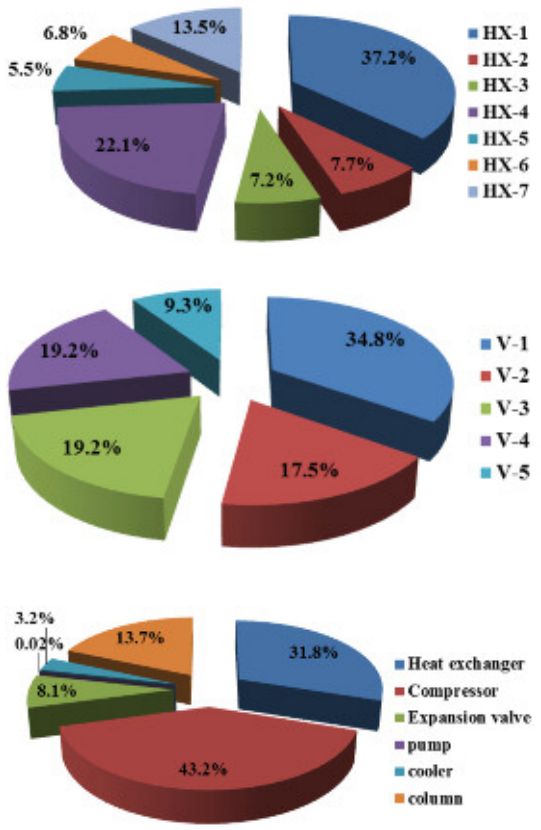

Figure 3. Distribution of exergy destruction in the system equipment

5.2. Results of Exergoeconomic Analysis

Referring to the table 5, it can be seen that T1 tower that has a condenser and a reboiler has the highest purchase equipment cost (5220.84 k$). Compressor C-MR2 has the next highest PEC (3460 k$). Using the cost balance equations as well as auxiliary equations (Table 6), a linear set of equations is created. Unit exergy cost of the process streams are obtained by solving the above-mentioned set of equations (Table 7).

Table 7 shows that streams 32 and 33 have the highest cost rate (16.9737 $/GJ) and streams 11, 12 and 13 have the lowest cost rate (0.8491 $/GJ).

Table 7. Unit exergy cost of the process streams

Stream	$\dot{C}\left(\frac{\$}{hr}\right)\times 10^3$	$c\left(\frac{\$}{GJ}\right)$
1	78400	12.94
2	78410	12.938
3	78696	12.946
4	79258	12.973
5	79200	12.973
6	76044	12.98
7	3214	12.98
8	4947	1.022
9	5156	1.064
10	5224	1.064
11	2371	0.8491
12	2307	0.8491
13	2306	0.8491
16	2693	1.2395
17	2688	1.2395
18	2691	1.2395
19	2691	1.2396
20	2656	1.2396
21	2649	1.2396
22	4956	1.0219
23	155573	14.4255
24	156084	14.4293
25	156122	14.4241
26	156301	14.4255
27	156265	14.4255
28	75134	16.9737
29	754935	16.9731
30	75498	16.9710
31	75730	16.9671
32	76179	16.9737
33	76141	16.9737

Table 8 presents the thermoeconomic parameters of the process components. Y_D is the amount of exergy destruction of each component with respect to the input fuel to the entire process. In this way, compressor C-MR2 has the highest exergy destruction (37.93%) and drum D-1 has the lowest exergy destruction (0.004%)

Table 8. Results of exergy and exergoeconomic analysis of the modified MFC process

Component	$\dot{E}_F(kW)$	$\dot{E}_P(kW)$	$\dot{E}_D(kW)$	$\dot{C}_F\left(\frac{\$}{hr}\right)$	$\dot{C}_P\left(\frac{\$}{hr}\right)$	$\dot{C}_D\left(\frac{\$}{hr}\right)$	$\dot{Z}\left(\frac{\$}{hr}\right)$	$Y_D(\%)$	$r(\%)$	$f(\%)$
HX-1	7758	2536	5222	34	53	18.99	19.01	11.17	37.4	50.1
HX-2	13323	12241	1082	692	696	3.79	3.79	2.31	94	49.6
HX-3	16478	15465	1012	1007	1012	7.84	4.84	2.16	7.06	49.9
HX-4	20769	17679	3090	63	67	4.25	4.28	6.61	25.34	50
HX-5	1073	293	780	2689	2693	4.79	4.25	1.66	72.5	47
HX-6	1564	612	952	3	7	4.25	4.29	2.03	0.014	49
HX-7	1347729	1345391	1897	4947	4956	8.59	4.26	4.05	0.011	33.1
Cooler1	1235721	1235512	209	75494	75494	0.041	0.046	0.44	0.017	50.2
Cooler2	3005978	3004771	1207	15684	15684	0.042	0.043	2.58	0.042	50.13
C-MR1	3013445	1235721	1328	75215	75494	7108	278.78	2.84	0.48	3.7
C-MR2	3013445	2995718	17727	155573	156216	642.78	378.57	37.93	0.3	37.1
Pump1	1345789	1345799	9.7	2421	2431	10	10	0.020	0.016	50.01
D-1	1695852	1695850	2	79201	79259	58.49	0.16	0.004	0.074	0.27
T1	1385394	1379364	6029	4485	5065	580.26	580.26	18.47	13.43	50.06

There is a specific procedure for thermoeconomic analysis and diagnosis of thermal cycles as mentioned below:

First off, all of the components are sorted in descending order, based on their importance. The relative importance of each component is evaluated by the sum of $\dot{C}_D$ and $\dot{Z}$. As it can be seen in the table 9 below, compressor C-MR1 has the highest value (7386.78 $/hr)

Table 9. Components, based on their importance

Component	$\dot{C}_D\left(\frac{\$}{hr}\right)+\dot{Z}\left(\frac{\$}{hr}\right)$
HX-1	38
HX-2	7.58
HX-3	12.68
HX-4	8.53
HX-5	9.04
HX-6	8.54
HX-7	12.85
Cooler1	0.087
Cooler2	0.085
C-MR1	7386.78
C-MR2	1021.35
Pump1	20
D-1	58.65
T1	1160.52

Components are arranged in table 9, based on their relative importance and cost. In order to improve the system performance, it is more advantageous to work on the components with highest cost value. Contrary to the exergy analysis, in the exergoeconomic diagnosis, the impact of the components on the process costs can be revealed.

Exergoeconomic factor (f) determines the relative importance of each component in the total cost of the system. If the exergoeconomic factor is high, then it should be checked whether it is economical to decrease the capital cost of the component or not. This is because, for these components, the initial investment cost is so high that their economic justification is in doubt. Table 10 shows the exergoeconomic factor of the process components. As it can be seen, cooler 1 and cooler 2 have the greatest Exergoeconomic factor (50.2% and 50.13% respectively). In these coolers, the initial capital costs are high and maybe using simpler and cheaper equipment is more economical.

If the exergoeconomic factor of a component is too small, its efficiency should be increased even if its initial cost grows larger. This is because, in such components, low efficiency imposes a high cost to the system. In Table 10 the components are arranged based on the value of exergoeconomic factor. As it can be observed, drum D-1 and compressor C-MR1 with 0.27% and 3.7% have the lowest exergoeconomic factor. These components should be preferably be replaced with more efficient components since they have imposed relatively high cost to the entire system.

Table 10. Exergoeconomic factor of the components

Component	F(%)
Cooler1	50.2
Cooler2	50.13
HX-1	50.1
T1	50.06
Pump1	50.01
HX-4	50
HX-3	49.9
HX-2	49.6
HX-6	49
HX-5	47
C-MR2	37.1
HX-7	33.1
C-MR1	3.7
D-1	0.27

In Fig.4, the effects of increasing the number of trays of column T1 on hot utility and exergoeconomic factor are shown. According to this figure, the highest exergoeconomic factor occurs when the number of trays is 6. Further increasing in the number of trays slightly decreases hot utility consumption. Furthermore, it results in lower exergoeconomic factor. As a result, the optimum number of trays is chosen to be 6.

Important characteristics of towers generally include reflux ratio, bottom feed ratio and purity of output streams. One of the design parameters of tower, considered in this research, is the purity of ammonia in output stream of the top of the tower. This parameter is chosen to be 99.9%

The second characteristic is bottom feed ratio which is defined as the ratio of the bottom product stream to the feed stream. The optimum value of this characteristic is obtained, with the sensitivity analysis, through the following procedure. Aspen-Hysys design software is employed for this purpose. To generate 28.25 MW cooling load n ammonia-water absorption system, different bottom feed ratios was examined. Reducing bottom feed ratio will result to a major decrease in feed stream mass flow rate. In this way, a reduction in bottom feed ratio from 0.94 to 0.78 will cause the feed stream mass flow rate to become 25% of its initial value. This means that a major portion of absorption refrigeration system becomes smaller. This will lead to a considerable decrease in the refrigeration cycle costs. On the other hand, as it can be seen from Fig.5, the rate of change in hot and cold utilities is small in comparison with the decrease in feed stream mass flow rate. In fact, as the bottom feed ratio decrease to 0.88, hot and cold utilities experience a marginal decrease but further reduction of the bottom feed ratio will cause hot and cold utilities to have a small increase. As a result, it is concluded that a reduction in bottom feed ratio is economically profitable. It should be mentioned that there is a limitation hereupon and that is the temperature of reboiler. As the bottom feed ratio decreases, the water content in bottom product increases, consequently the temperature of reboiler increases. Since the maximum temperature of reboiler can be 185 ^{C}, the minimum amount of bottom feed ratio would be 0.86. Choosing this value for bottom feed ratio will maximize exergetic efficiency.

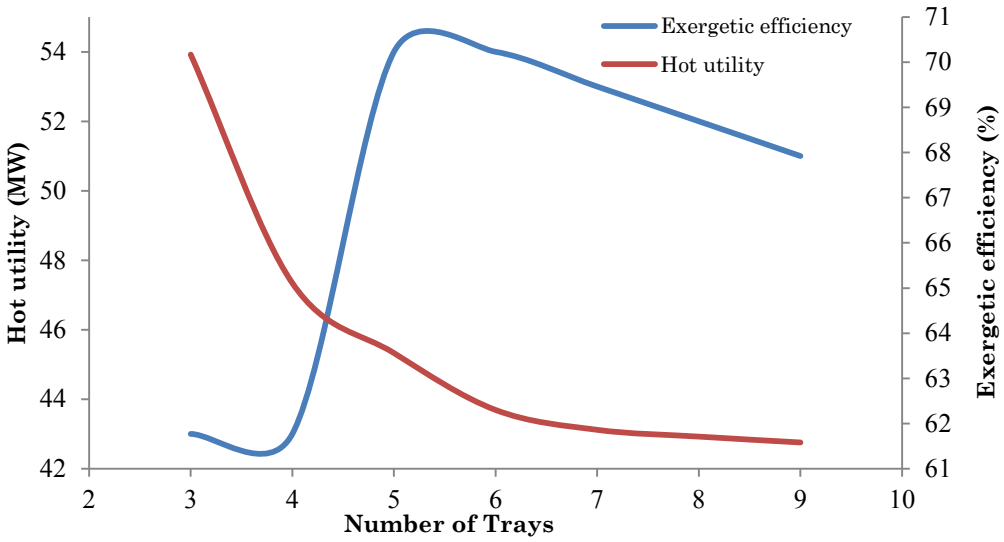

Figure 4. Variation of hot utility and exergoeconomic factor with respect to number of trays in T1 column

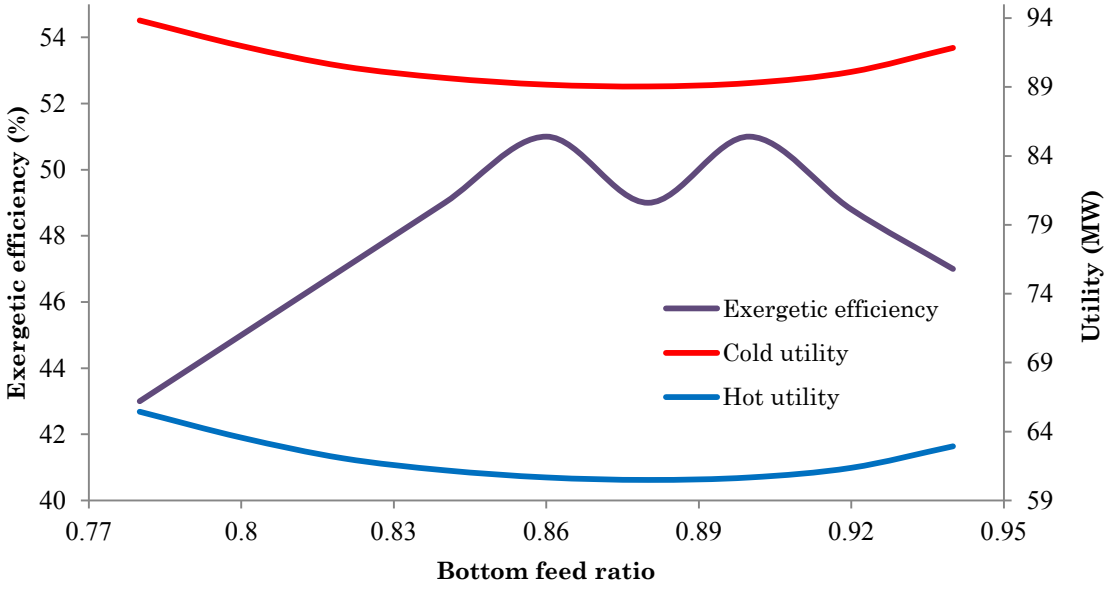

Figure 5. Variation of utility and exergoeconomic factor with respect to bottom feed ratio in T1 column

6. Sensitivity Analyses

For selecting appropriate decision variables of the system it is necessary to capture the behavior of the objective function with respect to decision variables. Since much of the electrical energy consumption of the plant is related to the compressors, optimizing and reducing their exergy destruction will lead to a more economical operation of the entire system. In Fig.6, the change of exergy destruction and exergoeconomic factor of HX1 versus the compression ratio of compressor C-MR1 is displayed. It is seen that increasing pressure ratio of this compressor will lead to higher exergy destruction cost and lower exergoeconomic factor of HX1. On the other hand, as the pressure ratio increases, the required work of this compressor and consequently its exergy destruction cost increases with a higher rate than the other components.

Fig.7 illustrates the change of exergy destruction and exergoeconomic factor of HX6 versus the compression ratio of compressor C-MR1. Increasing pressure ratio of this compressor will decrease the exergy destruction cost and increase exergoeconomic factor. When the pressure ratio reaches to 13, change of exergy destruction cost and exergoeconomic factor will be marginal.

Effect of increasing compression ratio of compressor C-MR1 on exergy cost of LNG and exergetic efficiency is displayed on Fig.8. This increase will cause a reduction in exergetic efficiency and an increase in exergy cost of LNG. Fig.9 shows that with increasing the compression ratio of compressor C-MR2, both exergy cost of LNG and purchase equipment cost will increase, but the rate of increase in purchase equipment cost is higher.

Finally, Fig.10 shows that cost of exergy destruction increases and exergoeconomic factor decreases as the compression ratio in compressor C-MR2 increases. Again, as the pressure ratio increases, the required work of this compressor and consequently its exergy destruction cost increases with a higher rate than the other components.

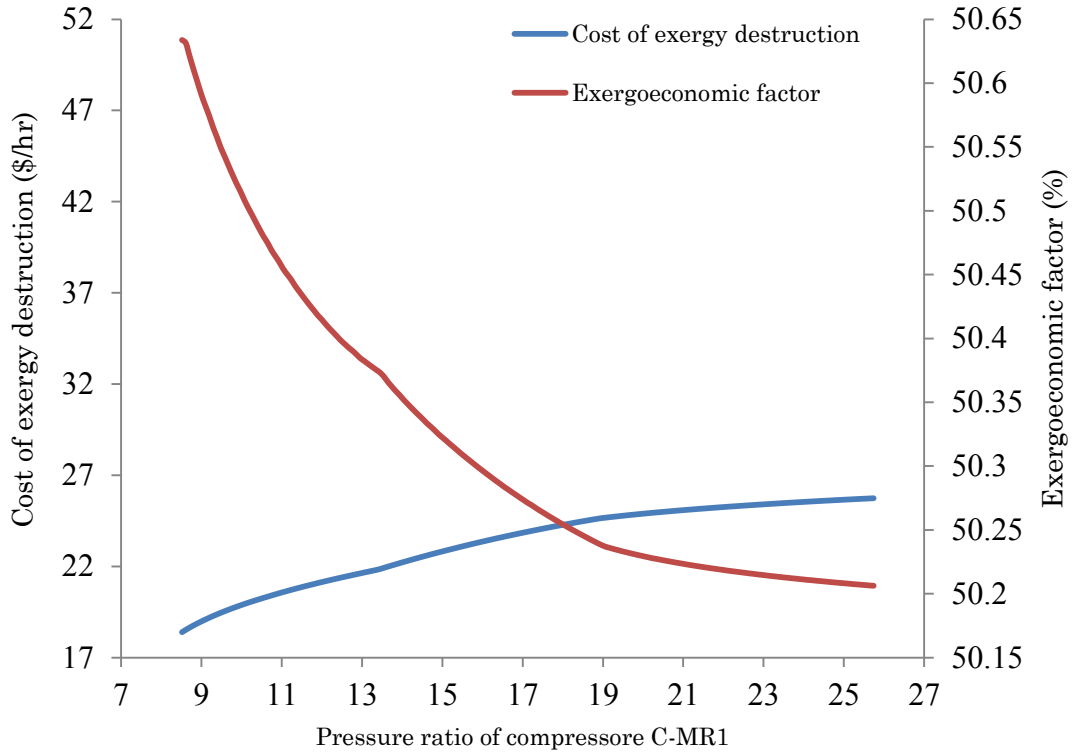

Figure 6. Variation of exergy destruction and exergoeconomic factor of HX1 with respect to compression ratio in C-MR1compressor

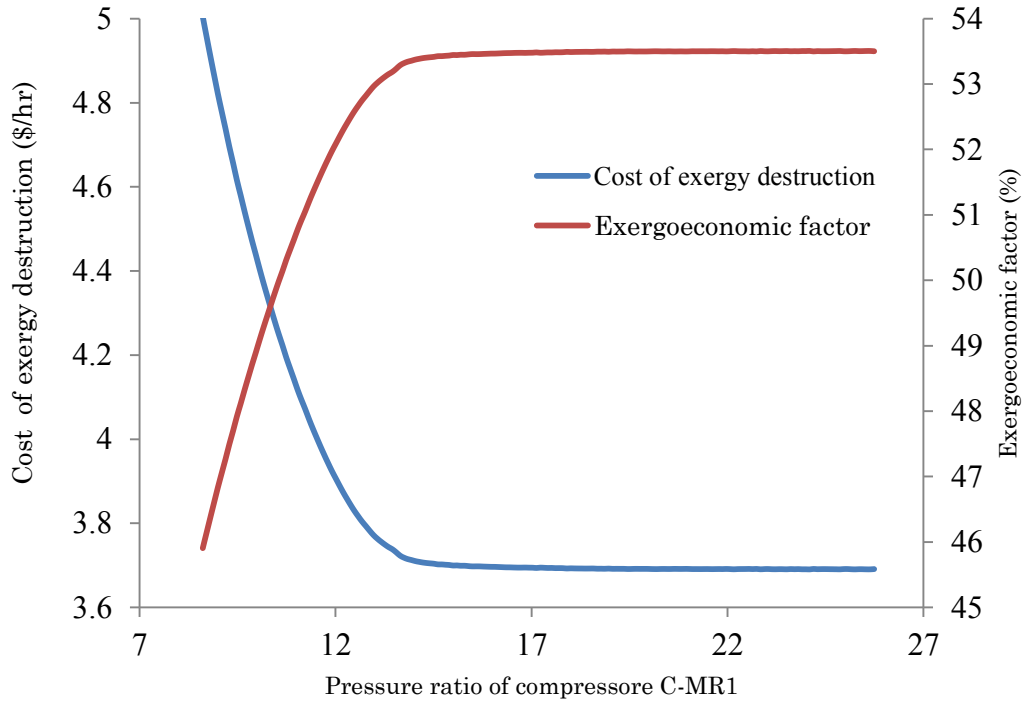

Figure 7. Variation of exergy destruction and exergoeconomic factor of HX6 with respect to compression ratio in C-MR1compressor

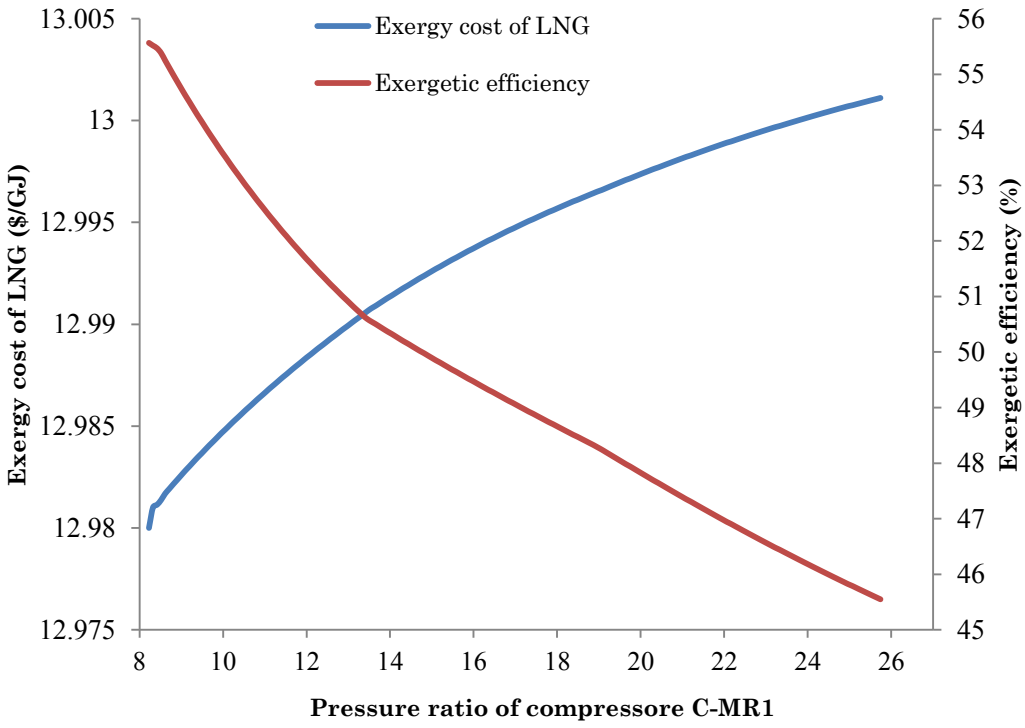

Figure 8. Variation of exergy cost of LNG and exergetic efficiency with respect to the compression ratio in C-MR1compressor

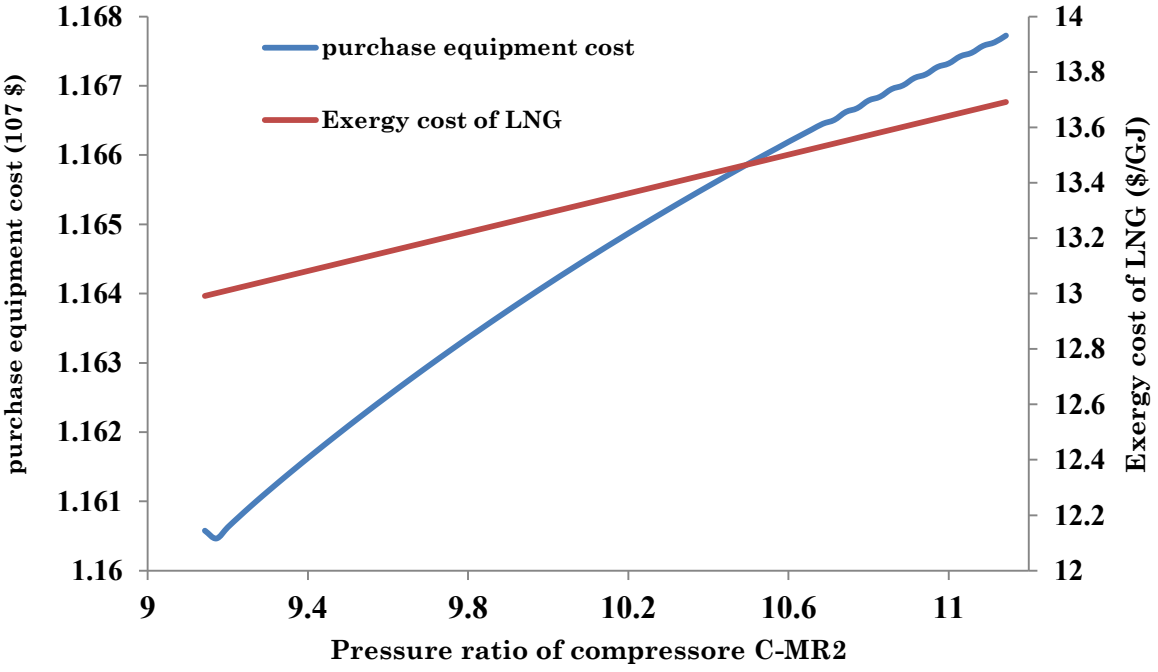

Figure 9. Variation of the exergy cost of LNG and purchase equipment cost with respect to compression ratio in C-MR2compressor

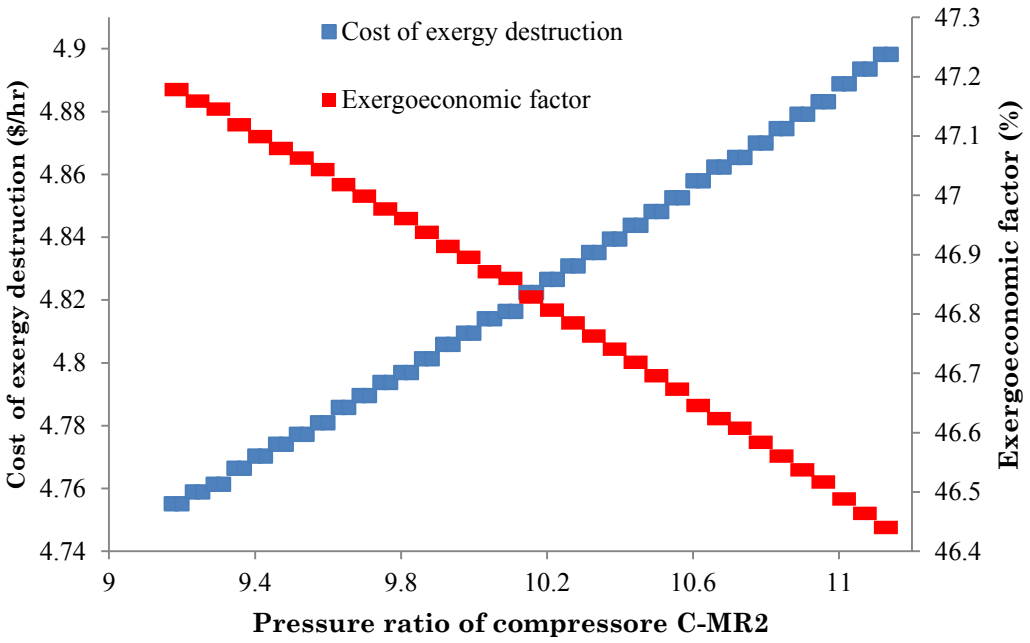

Figure 10. Variation of cost of exergy destruction and exergoeconomic factor of HX6 with respect to compression ratio in C-MR2 compressor

7. Integrated Gasification Process for Producing Synthesis Gas

In this paper, feed of Fischer Tropsch and generating of power are supplied using synthesis gas. The method of producing synthesis gas of process is carried out using gasification. The feed of gasification unit in this paper is coal. For simulating of integrated cogeneration of power, heating, and liquid fuels using gasification of feedstock like coal, the following operation units are developed. These units are consists of:

1- Sizing of the coal
2- Gasification unit
3- Air Separation (ASU)
4- Gas cleaning unit
5- Combined cycle power generation
6- Fischer Tropsch (FT)

Fig.11 shows schematic of the process. In this figure, the main units and connection of process streams and utilities are shown. The main steps are presented as follows:

Coal in sizing step is mixed with water to achieve the appropriate size for gasification process by crushing and screening operations. Finally, the slurry of coal for the production of synthesis gas is entered into the gasification section.

Gasification process requires oxygen, and required oxygen is supplied from the air separation unit (ASU). In this unit, air after initial treatment turns into nitrogen and oxygen. Required oxygen purity of process must be suitable for gasification process.

Coal-Water slurry with oxygen by purity of 95% are mixed in gasification unit and turns into synthesis gas with low heating value.

In cleaning unit, corrosive components such as sulfides, nitrides and dusts are separated from the production synthesis gas. Rehabilitation of rich H2S from acid gas removal system to produce sulfur will be sent to the Claus unit.

The produced synthesis gas is entered into the Fischer-Tropsch unit and is converted to fuel. Fischer-Tropsch syngas unit is the main unit of GTL, and its reactor is considered as heart in the process. Reaction in the conversion reactor produces a significant amount of water. The heavy components are separated in the Splitter100 and the produced water is separated in Splitter101. Part of the unreacted gases were returned by a backflow into the reactor, and produced hydrocarbons are transmitted to the quality improvement unit. Fig.11 shows the structure of the cogeneration power, heat and liquid fuel using synthesis gas method from gasification process. The reaction, occurred in the reactor, leads to producing considerable amount of water. The water by absorbing the released heat from reaction and exiting from reactor is entered into the splitter 101. A considerable

amount of produced heat by reaction is exited which has had high energy. On the other hand, the reactor must have a constant temperature and it is done with the water cycle within a shell around the reactor. The shell is shown Fig.11 along with the exchanger HX12.

Stream of Water 1 at the temperature of 25 ºC and pressure of 500 kPa is flown into the P101 pump and as stream of 601 at the pressure of 3200 kPa and temperature of 25.12 ºC is mixed with water stream exited from Splitter101 at the pressure of 3200 kPa and temperature of 220 ºC.

Stream of 604 at the temperature of 640.8 ºC and pressure of 100 bar is employed for pre-heating of mixture of natural gas, oxygen and water vapor in the HX10. Stream of 605 at the temperature of 508.6 ºC and pressure of 100 bar is entered into a steam turbine and with generation of power using stream of 606 at the temperature of 207 ºC and pressure of 500 kPa is exited. Almost 18% of the 606 as stream of 607 with the loss of 56.71 kW in heat exchanger of HX11 can provide the amount of heat required for Splitter100. Stream 608 with the loss of 6605 kW in the heat exchanger of HX13 can supply the amount of heat required for Splitter101. Stream of 609 at the temperature of 153.4 ºC and pressure of 500 kPa is mixed with stream of 613 which is at the temperature of 261.6 ºC and pressure of 500 kPa. The mixed stream i.e. stream of 614 is entered into the HX14. Stream of 614 after absorbing heat from the reactor Fischer-Tropsch (stream 107) is exited from exchanger HX14. Stream of 610 at the temperature and pressure of 159.8 ºC and 500 kPa as a hot steam is entered into the reboiler of separation tower of absorption refrigeration cycle and supplied required heating as much as 21350 kW. Approximately 66% of the stream of 611 as stream of water1 is used to provide closed cycle system. Integrated structure, presented in Fig.11, is employed for supplying power and hear of integrated structure of LNG production.

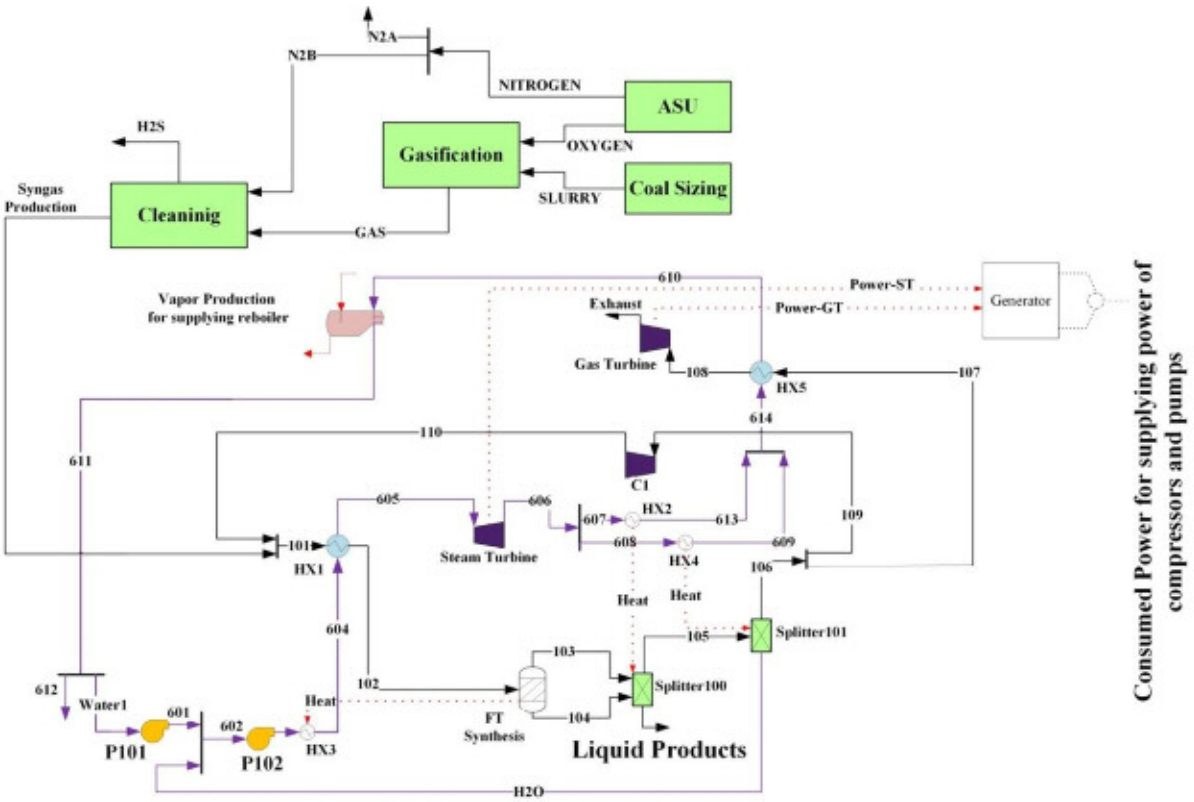

Figure 11. Schematic of integrated structure of CHP and liquid fuels from gasification of feedstock with primary material of coal using Fischer-Tropsch synthesis

Table11 compares the specific consumption of electricity and the amount of ethane recovery of the integrated structure integrated with other structures in the published papers and patents.

Table12 compares specifications for design of simulated ammonia water cycle in aspen hysys softwar with presented data in Amidpour et al for ammonia water cycle.

Table 11. Comparison of present study with other papers and patents in the industry

	refrigeration system	Number of compressors	Number of towers	Number of heat exchangers	Ethane recovery (%)	SP (kWh/kg LNG)	Comparison
Present study	AR-MR2	6	1	10	-	0.179	-
Ghorbani et al. design	MFC	7	2	4	92	0.343	0.32
Ghorbani et al. design	C3-MR	5	2	5	92	0.359	*
Ghorbani et al. design	AR-MR1	3	3	3	91.6	0.25	*
	DMR	7	2	4	92	0.351	*
	C3-MR	5	2	4	92	0.359	*
APCI	C3-MR	-	1	-	-	-	-
ConocoPhillips design	cascade	4	1	9	-	-	-
ConocoPhillips design	cascade	3	2	9	-	-	-
Ortloff	-	5	2 and 1	5	42-95	0.28-0.43, 0.5	~ 0.35
Fluor Technologies alternatives	pure-MR	-	2-3	3	25-85	-	-

Table 12. Comparison of specifications for design of simulated ammonia water cycle in aspen hysys softwar with presented data in Amidpour et al for ammonia water cycle

	Relative Error	Amidpour et al	Presented data
Evaporator heating load Q_{evap} (kW)		166	169.1
Cycle performance coefficient	1.83%	0.615	0.622
Low pressure (bar)	0%	2.596	2.596
High pressure (bar)	0%	15.28	15.28
Condenser cooling load Q_{cond} (kW)	-3.17%	178.1	172.2
Absorption cooling load Q_{abs} (kW)	-1.58%	215.1	211.7
Concentration of ammonia in lean solution (mas%)	-4.01%	26.91	25.88
Concentration of ammonia in rich solution (mas%)	0%	33	33
Heating load in generator Q_{gen} (kW)	-1.8%	277.8	272.6

8. Conclusions

In this study, a novel mixed fluid cascade natural gas liquefaction process was studied with exergoeconomic analysis method. The results are summarized as follows:

1- Highest exergy destruction in the process belongs to the compressors. As the exergy destruction in the compressors directly affects the required power in the process, its reduction can drastically decreases the operating costs of the plant.

2- Exergoeconomic shows that water coolers, heat exchanger HX-1, tower T1 and pump P1 have the highest exergoeconomic factor, respectively. Consequently, it can impose high initial investment cost to the plant. It is advisable to replace these equipment with cheaper ones. Efficiency improvement of compressors C-MR1 and C-MR2 should be considered, even though that will probably result in higher initial investment. Heat exchangers HX-5 and HX-6 are the next candidates for improvement.

3- Sensitivity analysis shows that the optimum number of trays is 6, and the best value for bottom feed ratio is 0.86. These values will result in best exergetic efficiency and optimum utility consumption.

Nomenclature

Q	Heat duty (kW)
r	Relative cost difference (%)
c	unit exergy cost ($/kJ)
$\dot{C}$	exergy cost rate ($/h)
$\dot{m}$	Mass flow rate (kg/s)
r_{FC}	annual escalation rate for the fuel cost
ROI	Return on investment
c_w	Unit cost of the generated electricity ($/kW)
e	Specific flow exergy (kJ/kgmole)
$\dot{E}$	Exergy rate (kW)
Ex	Exergy (kW)
F	Exergoeconomic factor (%)
I	Irreversibility (kW)
ieff	average annual discount rate
j	jth year of operation
m	Number of cold streams
n	Number of hot streams
r_{OM}	Annual escalation rate for the O&M cost
W	Power (kW)
$\dot{W}$	Exergy destruction ratio

Abbreviations

AC	Air cooler
TCR	Total capital recovery
TRR	Total revenue requirement
C	Compressor
MR	Mixed Refrigerant
V	Expansion valve
BL	book life
COP	Coefficient of Performance
NG	Natural Gas
LNG	Liquefied Natural Gas
MFC	Mixed Fluid Cascade
SPC	Specific Power Consumption
MR	Mixed Refrigerant
F	Phase separator
C	Cold box
P	Pump
E	Exchanger
K	Compressor
V	Valve
CC	Carrying charge
CRF	capital recovery factor
OMC	Operating and maintenance cost
PEC	Purchase equipment cost ($)
FC	Fuel cost ($/s)
CRC	compression refrigeration cycle

subscripts

a	air
av	average
cw	Cooling water
f	Fuel
p	product
0	index for first year of operation
a	Air
c	Cold
D	Destruction
h	Hot
i	Inlet
k	kth component
L	levelized

Superscripts

CI	Capital investment
OM	Operating and maintenance

References

Adams, P. W. R., & McManus, M. C. (2014). Small-scale biomass gasification CHP utilisation in industry: Energy and environmental evaluation. *Sustainable Energy Technologies and Assessments, 6*, 129-140. doi:https://doi.org/10.1016/j.seta.2014.02.002

Alabdulkarem, A., Mortazavi, A., Hwang, Y., Radermacher, R., & Rogers, P. (2011). Optimization of propane pre-cooled mixed refrigerant LNG plant. *Applied*

Thermal Engineering, 31(6), 1091-1098.

Amidpour, M., Hamedi, M., Mafi, M., Ghorbani, B., Shirmohammadi, R., & Salimi, M. (2015). Sensitivity analysis, economic optimization, and configuration design of mixed refrigerant cycles by NLP techniques. *Journal of Natural Gas Science and Engineering, 24*, 144-155.

Aneke, M., Agnew, B., Underwood, C., & Menkiti, M. (2012). Thermodynamic analysis of alternative refrigeration cycles driven from waste heat in a food processing application. *international journal of refrigeration, 35*(5), 1349-1358.

Avidan, A. A., Gardner, R. E., Nelson, D., Borrelli, E. N., & Rethore, T. J. (1997). LNG links remote supplies and markets. *Journal Name: Oil and Gas Journal; Journal Volume: 95; Journal Issue: 22; Other Information: PBD: 2 Jun 1997*, Medium: X; Size: pp. 54-59.

Bahadori, A. (2014). Chapter 13 - Liquefied Natural Gas (LNG) *Natural Gas Processing* (pp. 591-632). Boston: Gulf Professional Publishing.

Bejan A, T. G., Moran M. (1996). *Thermal Design and Optimization*: Wiley.

Berger, E., Forg, W., Heiersted, R., & Paurola, P. (2003). The Snohvit Project: The MFC®(Mixed Fluid Cascade) Process for the first European Baseload LNG Production Plant. *Linde Technology*, 12-23.

Brant, B., Brueske, S., Erickson, D., & Papar, R. (1998). New waste-heat refrigeration unit cuts flaring, reduces pollution. *Oil and Gas Journal, 96*(20).

Bruno, J., Vidal, A., & Coronas, A. (2006). Improvement of the raw gas drying process in olefin plants using an absorption cooling system driven by quench oil waste heat. *Energy Conversion and Management, 47*(1), 97-113.

Dai, Y., Wang, J., & Gao, L. (2009). Exergy analysis, parametric analysis and optimization for a novel combined power and ejector refrigeration cycle. *Applied Thermal Engineering, 29*(10), 1983-1990. doi:http://dx.doi.org/10.1016/j.applthermaleng.2008.09.016

Dispenza, A., La Rocca, V., Messineo, A., Morale, M., & Panno, D. (2013). Absorption equipment for energy savings: A case study in Sicily. *Sustainable Energy Technologies and Assessments, 3*, 17-26.

dos Santos, I. F. S., Vieira, N. D. B., Barros, R. M., Filho, G. L. T., Soares, D. M., & Alves, L. V. (2016). Economic and CO2 avoided emissions analysis of WWTP biogas recovery and its use in a small power plant in Brazil. *Sustainable Energy Technologies and Assessments, 17*, 77-84. doi:https://doi.org/10.1016/j.seta.2016.08.003

Ghaebi, H., Karimkashi, S., & Saidi, M. (2012). Integration of an absorption chiller in a total CHP site for utilizing its cooling production potential based on R-curve concept. *International Journal of Refrigeration, 35*(5), 1384-1392.

Ghorbani, B., Hamedi, M.-H., & Amidpour, M. (2016). Exergoeconomic Evaluation of an Integrated Nitrogen Rejection Unit with LNG and NGL Co-Production Processes Based on the MFC and Absorbtion Refrigeration Systems. *Gas Processing, 4*(1), 1-28.

Ghorbani, B., Hamedi, M.-H., Amidpour, M., & Shirmohammadi, R. (2017). Implementing absorption refrigeration cycle in lieu of DMR and C3MR cycles in the integrated NGL, LNG and NRU unit. *International Journal of Refrigeration, 77*, 20-38.

Ghorbani, B., Hamedi, M.-H., Shirmohammadi, R., Hamedi, M., & Mehrpooya, M. (2016). Exergoeconomic analysis and multi-objective Pareto optimization of the C3MR liquefaction process. *Sustainable Energy Technologies and Assessments, 17*, 56-67.

Ghorbani, B., Hamedi, M., Shirmohammadi, R., Mehrpooya, M., & Hamedi, M.-H. (2016). A novel multi-hybrid model for estimating optimal viscosity correlations of Iranian crude oil. *Journal of Petroleum Science and Engineering, 142*, 68-76. doi:https://doi.org/10.1016/j.petrol.2016.01.041

Ghorbani, B., Mafi, M., Shirmohammadi, R., Hamedi, M.-H., & Amidpour, M. (2014). Optimization of operation parameters of refrigeration cycle using particle swarm and NLP techniques.

Journal of Natural Gas Science and Engineering, 21, 779-790.

Han, W., Sun, L., Zheng, D., Jin, H., Ma, S., & Jing, X. (2013). New hybrid absorption–compression refrigeration system based on cascade use of mid-temperature waste heat. *Applied Energy, 106*, 383-390.

Hasan, M., Karimi, I., & Alfadala, H. (2009). *Optimizing compressor operations in an LNG plant*. Paper presented at the Proceedings of the 1st annual gas processing symposium.

Hasan, M. F., Razib, M. S., & Karimi, I. (2009). Optimization of compressor networks in LNG operations. *Computer Aided Chemical Engineering, 27*, 1767-1772.

Hwang, J.-H., Roh, M.-I., & Lee, K.-Y. (2013). Determination of the optimal operating conditions of the dual mixed refrigerant cycle for the LNG FPSO topside liquefaction process. *Computers & Chemical Engineering, 49*, 25-36.

Jensen, J. B., & Skogestad, S. (2006). Optimal operation of a mixed fluid cascade LNG plant. In W. Marquardt & C. Pantelides (Eds.), *Computer Aided Chemical Engineering* (Vol. Volume 21, pp. 1569-1574): Elsevier.

Kalinowski, P., Hwang, Y., Radermacher, R., Al Hashimi, S., & Rodgers, P. (2009). Application of waste heat powered absorption refrigeration system to the LNG recovery process. *international journal of refrigeration, 32*(4), 687-694.

Kanoğlu, M. (2001). Cryogenic turbine efficiencies. *Exergy, An International Journal, 1*(3), 202-208.

Kaynakli, O., Saka, K., & Kaynakli, F. (2015). Energy and exergy analysis of a double effect absorption refrigeration system based on different heat sources. *Energy Conversion and Management, 106*, 21-30. doi:http://dx.doi.org/10.1016/j.enconman.2015.09.010

Khan, E. U., Mainali, B., Martin, A., & Silveira, S. (2014). Techno-economic analysis of small scale biogas based polygeneration systems: Bangladesh case study. *Sustainable Energy Technologies and Assessments, 7*, 68-78.

Kotas, T. J. (2013). *The exergy method of thermal plant analysis*: Elsevier.

Mehrpooya, M., Omidi, M., & Vatani, A. (2016). Novel mixed fluid cascade natural gas liquefaction process configuration using absorption refrigeration system. *Applied Thermal Engineering, 98*, 591-604. doi:http://dx.doi.org/10.1016/j.applthermaleng.2015.12.032

Morosuk, T., Tesch, S., Hiemann, A., Tsatsaronis, G., & Bin Omar, N. (2015). Evaluation of the PRICO liquefaction process using exergy-based methods. *Journal of Natural Gas Science and Engineering, 27, Part 1*, 23-31. doi:http://dx.doi.org/10.1016/j.jngse.2015.02.007

Mortazavi, A., Somers, C., Alabdulkarem, A., Hwang, Y., & Radermacher, R. (2010). Enhancement of APCI cycle efficiency with absorption chillers. *Energy, 35*(9), 3877-3882.

Petrakopoulou, F., Tsatsaronis, G., & Morosuk, T. (2013). Evaluation of a power plant with chemical looping combustion using an advanced exergoeconomic analysis. *Sustainable Energy Technologies and Assessments, 3*, 9-16. doi:http://dx.doi.org/10.1016/j.seta.2013.05.001

Raj, R., Suman, R., Ghandehariun, S., Kumar, A., & Tiwari, M. K. (2016). A techno-economic assessment of the liquefied natural gas (LNG) production facilities in Western Canada. *Sustainable Energy Technologies and Assessments, 18*, 140-152.

Rodgers, P., Mortazavi, A., Eveloy, V., Al-Hashimi, S., Hwang, Y., & Radermacher, R. (2012). Enhancement of LNG plant propane cycle through waste heat powered absorption cooling. *Applied Thermal Engineering, 48*, 41-53.

Salomón, M., Gomez, M. F., & Martin, A. (2013). Technical polygeneration potential in palm oil mills in Colombia: A case study. *Sustainable Energy Technologies and Assessments, 3*, 40-52. doi:https://doi.org/10.1016/j.seta.2013.05.003

Sheikhi, S., Ghorbani, B., Shirmohammadi, R., & Hamedi, M.-H. (2014). Thermodynamic and Economic Optimization of a Refrigeration Cycle for Separation Units in the Petrochemical Plants Using Pinch

Technology and Exergy Syntheses Analysis. *Gas Processing Journal, 2*(2), 39-52. Retrieved from http://uijs.ui.ac.ir/gpj/browse.php?a_code=A-10-350-1&slc_lang=en&sid=1

Sheikhi, S., Ghorbani, B., Shirmohammadi, R., & Hamedi, M.-H. (2015). Advanced Exergy Evaluation of an Integrated Separation Process with Optimized Refrigeration System. *Gas Processing Journal, 3*(1), 1-10.

Shirmohammadi, R., Ghorbani, B., Hamedi, M., Hamedi, M.-H., & Romeo, L. M. (2015). Optimization of mixed refrigerant systems in low temperature applications by means of group method of data handling (GMDH). *Journal of Natural Gas Science and Engineering, 26*, 303-312.

Stockmann, R., Forg, W., Bolt, M., Steinbauer, M., Pfeiffer, C., Paurola, P., . . . Sorensen, O. (2001). Method for liquefying a stream rich in hydrocarbons: Google Patents.

Táboas, F., Bourouis, M., & Vallès, M. (2014). Analysis of ammonia/water and ammonia/salt mixture absorption cycles for refrigeration purposes in fishing ships. *Applied Thermal Engineering, 66*(1), 603-611.

Venkatarathnam, G., & Timmerhaus, K. D. (2008). *Cryogenic mixed refrigerant processes*: Springer.

Waldmann, I. (2008). *Evaluation of process systems for floating LNG production units.* Paper presented at the Tekna conference.

Wang, R., & Oliveira, R. (2006). Adsorption refrigeration—an efficient way to make good use of waste heat and solar energy. *Progress in Energy and Combustion Science, 32*(4), 424-458.

Xu, X., Liu, J., Jiang, C., & Cao, L. (2013). The correlation between mixed refrigerant composition and ambient conditions in the PRICO LNG process. *Applied Energy, 102*, 1127-1136.

Xydis, G., Nanaki, E., & Koroneos, C. (2013). Exergy analysis of biogas production from a municipal solid waste landfill. *Sustainable Energy Technologies and Assessments, 4*, 20-28. doi:http://dx.doi.org/10.1016/j.seta.2013.08.003

Yan, X., Chen, G., Hong, D., Lin, S., & Tang, L. (2013). A novel absorption refrigeration cycle for heat sources with large temperature change. *Applied Thermal Engineering, 52*(1), 179-186.

Brostow, A.A. and M.J. Roberts, Integrated NGL recovery in the production of liquefied natural gas. 2006, Google Patents.

Roberts, M.J. and A.A. Brostow, Integrated NGL Recovery And Liquefied Natural Gas Production. 2010, Google Patents.

Ransbarger, W.L., Intermediate pressure LNG refluxed NGL recovery process. 2006, Google Patents.

Qualls, W., et al., Lng facility with integrated ngl extraction technology for enhanced ngl recovery and product flexibility. 2006, Google Patents.

Cuellar, K.T., et al., CO-PRODUCING LNG FROM CRYOGENIC NGL RECOVERY PLANTS. 2002.

Martinez, T.L., et al., Liquefied natural gas and hydrocarbon gas processing. 2014, Google Patents.

Mak, J. and C. Graham, Configurations and methods of integrated NGL recovery and LNG liquefaction. 2006, Google Patents

Ghorbani, B., Hamedi, M.-H., Amidpour, M., & Mehrpooya, M. (2016). Cascade refrigeration systems in integrated cryogenic natural gas process (natural gas liquids (NGL), liquefied natural gas (LNG) and nitrogen rejection unit (NRU)). Energy, 115, 88-106.

Ghorbani, B., Hamedi, M.-H., & Amidpour, M. (2016). Development and optimization of an integrated process configuration for natural gas liquefaction (LNG) and natural gas liquids (NGL) recovery with a nitrogen rejection unit (NRU). Journal of Natural Gas Science and Engineering, 34, 590-603.